

Peculiarities of the transitions to synchronization in coupled systems with amplitude death

V. Astakhov,¹ S. Koblyanskii,² A. Shabunin,² and T. Kapitaniak³

¹Radiotechnical Department, Saratov State Technical University,

Polytechnicheskaya 77, Saratov 410054, Russia

²Radiophysics and Nonlinear Dynamics Department, Saratov State University,

Astrakhanskaya 83, Saratov 410026, Russia

³Division of Dynamics, Technical University of Lodz, Stefanowskiego 1/15, Lodz 90-924, Poland

(Received 25 October 2010; accepted 13 May 2011; published online 24 June 2011)

The paper presents the results of the study of the sequences of bifurcation leading to the synchronization and amplitude death in a system of two dissipatively coupled self-sustained oscillators with inertial nonlinearity. Two types of synchronization tongues have been identified. In one of them phase locking regions exist where the synchronization is achieved by the saddle-node bifurcation and regions where the transition to synchronization leads through Neimark-Sacker bifurcation. In the second type of the tongues there are only phase locking regions. It has been shown that for a weak non-identity of the system parameters, the first type tongues merge together. The transition between the synchronization tongues can occur without bifurcations, i.e., transition between the synchronized regimes with different periods of oscillations can occur gradually.

© 2011 American Institute of Physics. [doi:10.1063/1.3597643]

Recent investigations have shown that the coupled systems have a great potential in a large amount of application areas ranging from physics and engineering to economy and biology. In this paper we study the dynamics of two linearly, dissipatively coupled self-sustained oscillators with inertial non-linearity, which demonstrates period doubling bifurcations. We give evidence that the system behavior is characterized by a number of peculiarities (unexpected events), such as: (i) the existence of synchronization tongues in which the regions with different synchronization mechanism exist, (ii) the creation of the infinitely long band between the regions of amplitude death and quasiperiodic behavior (this phenomenon has been observed previously in different systems,¹⁸ but we identify its bifurcation mechanism), (iii) the existence of tongues which are closed on both sides (at the bottom and at the top). We show that these peculiarities allow smooth transition between the synchronization tongues with different periods of oscillations. We argue that the described phenomena are robust and can be observed for the wide range of system parameters.

the result of supercritical Andronov-Hopf bifurcation a stable limit cycle is born from an equilibrium. Then, with further parameters' change the cycle undergoes Neimark-Sacker bifurcation, after which it loses stability and gives birth of a stable two-dimensional torus in its neighborhood. Moving along Neimark-Sacker bifurcation line on two-dimensional parameters' plane we observe the synchronization domains (Arnolds' tongues), the boundaries of which are formed by the lines of saddle-node bifurcations of the resonance cycles. The last ones are saddle and stable limit cycles located on two-dimensional torus. Arnold's tongues lean on the line of Neimark-Sacker bifurcation and their sequence obeys Fairys' rule. The described sequence of the tongues forms the universal structure near the line of the torus birth. It repeats for mutual synchronization of weakly coupled self-sustained oscillators with different types of interaction, as well as for external synchronization by small harmonic force.

However, over the line of Neimark-Sacker bifurcation, the picture of synchronization becomes less universal and more complex. A large number of publications (see, e.g., Refs. 13–18) are devoted to the investigation of the global structure of synchronization regions in autonomous and non-autonomous systems.

Peculiarities of the behavior of interaction systems depend on both, the strength and the type of coupling. For e.g., if the conservative coupling is considered, both the synchronization phenomena and the multistability phenomena in the system of two van der Pol oscillators are observed.¹⁹ The bistability of synchronous regimes leads to the determined peculiarities of the bifurcational mechanism of the loss of synchronization.²⁰ If the dissipative coupling is considered, we can observe in two self-oscillations systems not only the mutual synchronization but the effect of amplitude

I. INTRODUCTION

Mutual synchronization is a fundamental property in nature, observed in a large number of interacting self-sustained oscillatory systems (see, e.g., monographs 4–10). The simplest case of synchronization is the synchronization of periodic oscillators, which has been intensively studied since the pioneering work of Hugenius.^{1,2} Typical chains of bifurcations which lead to synchronization are well-known (see, e.g., Ref. 11). Let us briefly remind the main points. First, in

death as well (see, e.g., Refs. 8, 12, 17–19). In this case the transitions from equilibria to quasiperiodic and synchronous oscillations are observed not only at a weak coupling but also at a strong coupling. However, as it will be demonstrated below, the weak coupling region and the strong coupling region can be distinguished by the corresponding structure of the bifurcation set in the space of control parameters in an essential manner. Because of it, the peculiarities of the transitions to synchronization in the coupled systems with amplitude death appear.

The phenomenon of oscillation quenching at increasing mutual coupling between self-excited systems with different natural frequencies was described first by Rayleigh in his fundamental work “The Theory of Sound.”³ At researching the mutual influence of the neighboring organ-pipes he found, that “when two organ-pipes of the same pitch stand side by side, complications ensue which do not unfrequently give trouble in practice. In extreme cases, the pipes may almost reduce one another to silence. Even when the mutual influence is more moderate, it may still go so far as to cause the pipes to speak in absolute unison, in spite of inevitable small natural differences.” So he observed both the synchronization and the oscillation quenching in dependence on the strength of the interaction between the systems. It is well-known (see, e.g., Ref. 8) that the oscillation quenching occurs because of the additional dissipation in the united system at inserting of coupling. The energy of the source of the united self-excited system does not compensate additional losses of energy in the channel of coupling. The mechanism of realization of the self-oscillation quenching can be different. Usually, three main mechanisms are distinguished:²⁵ a large detuning between natural frequencies at the strong coupling results in oscillation quenching,^{21,26–28} a time-delay in the coupling can lead to quenching,^{29–32} the coupling through dissimilar (or conjugate) variables in the system of identical oscillators can also lead to quenching.³³ The oscillation quenching can result in a homogeneous steady state or an inhomogeneous steady state in the ensemble of the coupled oscillators. In the first case, the phenomenon of oscillation quenching is distinguished as the amplitude death and the second case refers to the oscillations death.²⁵ The phenomenon of the oscillation quenching has a universal character and is observed in various fields, including acoustic systems,³ coupled chemical and biological oscillators,^{21,25,34} coupled electrochemical oscillators,³⁵ time-delay coupled thermo-optical oscillators,³⁶ and coupled electronic circuits.³⁷ Irrespective of the nature of the system, when it happens in phase space the steady state becomes stable as the result of supercritical or subcritical Andronov-Hopf bifurcation. The appearance of the oscillations death is associated with the pitchfork bifurcation.

The simplest model which demonstrates both the synchronization and the amplitude death phenomena is the one given by reduced van der Pole equations (also known as Landau-Stuart equation⁸). The phenomenon of amplitude death has been studied also in more realistic systems of different nature.^{21,22}

Despite the large scale of publications concerning the problems of the amplitude death phenomenon, some of the

questions still remain open. In particular, the bifurcational mechanisms of the transition between quasiperiodic oscillations and amplitude death regime have been considered only in the neighborhood of the main synchronization tongue (1:1) (Ref. 19). How this mechanism is transformed into other synchronization tongues with different rotation numbers is fairly less studied.

In this paper, we carry out the bifurcation analysis of the phenomena of synchronization and amplitude death in a wide region of parameters for different rotate numbers. The system under study is two dissipative coupled self-sustained oscillators with inertial non-linearity. The results are obtained by the software package for bifurcational analysis AUTO (Ref. 23). Our studies allow the identification of a number of peculiarities (unexpected events) such as: (i) the synchronization tongues in which the regions with different synchronization mechanism exist, (ii) the creation of the infinitely long band between the regions of amplitude death and quasiperiodic behavior, which has been observed also by other authors in different systems,¹⁸ but the bifurcation mechanism of this event is revealed first in this work, (iii) the tongues which are closed on both sides (at the bottom and at the top), (iv) the tongues which are merged at strong coupling. We give evidence that these peculiarities allow smooth transition between the synchronization tongues with different periods of oscillations. We argue that the described phenomena are robust and can be observed for the wide range of system parameters.

The paper is organized as follows. Section II introduces the model of the considered system. The bifurcations which occur in the neighborhood of the 1:1 principal resonance are described in Sec. III. Section IV presents the bifurcation scenario in the neighborhood of other resonances. In Secs. III and IV the cases of identical and nonidentical oscillators are considered. Finally, we summarize our results in Sec. V.

II. MODEL

We consider the bifurcational mechanisms of synchronization and amplitude death in the system of dissipatively coupled self-sustained oscillators with inertial nonlinearity. The dynamics of the system is described as follows:

$$\begin{aligned} \dot{x}_1 &= m_1 x_1 - p x_1 z_1 + p y_1 + \epsilon(x_2 - x_1), \\ \dot{y}_1 &= -x_1, \quad \dot{z}_1 = -g[z_1 - f(x_1)], \\ \dot{x}_2 &= m_2 x_2 - x_2 z_2 + y_2 + \epsilon(x_1 - x_2), \quad \dot{y}_2 = -x_2, \\ \dot{z}_2 &= -g[z_2 - f(x_2)], \end{aligned} \quad (1)$$

where $f(x_{1,2}) = \exp(x_{1,2}) - 1$, $x_{1,2}$, $y_{1,2}$, and $z_{1,2}$ are the dynamical variables, $m_{1,2}$, g , p and ϵ are the system parameters. Here $m_{1,2}$ are the system parameters which describe the birth of self-excited oscillations in both subsystems (that is Andronov-Hopf bifurcation in partial oscillator). g is the inertial parameter which in our studies has been fixed to the value $g = 0.2$. Parameter $p = \omega_1/\omega_2$ describes detuning between fundamental frequencies ω_1 and ω_2 of partial oscillators.

In the case of $\epsilon = 0$ both oscillators (subsystems) are uncoupled. For negative values of the parameters $m_{1,2}$ in both subsystems the fixed points $x_{1,2} = y_{1,2} = z_{1,2}$ are stable.

For $m_{1,2} = 0$ one observes supercritical Andronov-Hopf bifurcations in which stable limit cycles of self-excited oscillations are born. The amplitudes of these oscillations are proportional to \sqrt{m} . For small values of $m_{1,2}$ one observes quasi-harmonic oscillations. With the increase of $m_{1,2}$ the subsystems can demonstrate both periodic and chaotic oscillations. The route to the chaotic oscillations leads through the cascade of period-doubling bifurcations. The detailed analysis of the dynamics of the partial system with the nonlinear function $f(x) = 0.25(|x| + x)^2$ is given in Ref. 24. The partial system with nonlinearity $f(x) = \exp(x) - 1$ shows qualitatively the same behavior.

For $\epsilon \neq 0$ coupled system (1) shows rich bifurcational behavior. Depending on the system parameters one can observe the synchronization of periodic and chaotic self-oscillations, phase multistability, and the effects of amplitude death. In our studies we consider the occurrence of synchronization of periodic oscillations and amplitude death in the wide range of the system parameters ϵ and p , assuming that the subsystems exhibit self-oscillations of period one.

III. BIFURCATIONS IN THE NEIGHBORHOOD OF THE 1:1 RESONANCE

A. Synchronization of the systems with identical limit cycles

Let us consider the dynamics of two coupled identical (i.e., without additional mismatch of the excitation parameters $m_{1,2}$) oscillators. We fixed $m_1 = m_2 = m = 0.1$ and considered the dependence of the system (1) behavior on the parameters: ϵ and p . For the assumed value of m , partial oscillators (subsystems) show quasi-harmonic oscillations.

First, we follow the stable and unstable periodic orbits and their bifurcations in the principal 1:1 synchronization region. In Fig. 1 we present the bifurcation lines of the stable and unstable limit cycles and unstable fixed points in the principal 1:1 synchronization region. The synchronized oscillations exist in the regions *A* and *B*. These regions are

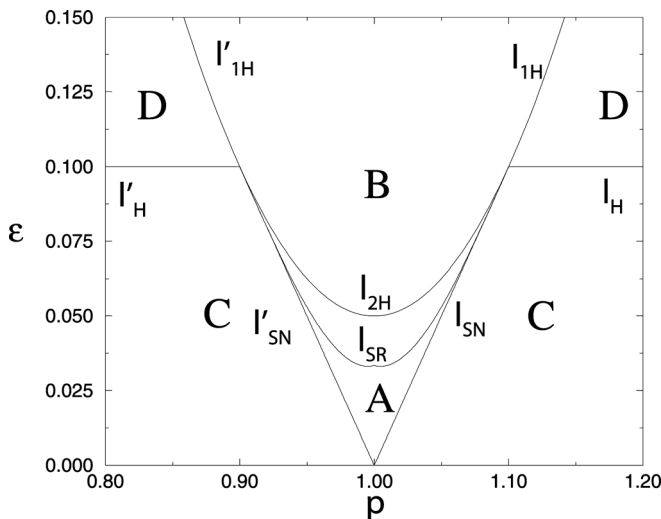


FIG. 1. Bifurcation diagram of the system (1) in the main area of synchronization region $S_{1:1}$ on the plane of control parameters ($\epsilon - p$) (coupling coefficient, detuning parameter): $m_1 = m_2 = 0.1, g = 0.2$.

surrounded by the regions of quasiperiodic oscillations *C* and amplitude death *D*. For the system parameters in region *A* bounded by the bifurcation lines I_{SN}, I'_{SN} , and I_{SR} , system (1) has unstable fixed point P_R , three saddle limit cycles C_S, C_P, C_R , and stable limit cycle C_N as shown in Figs. 2(a) and 2(b). The limit cycles represent the synchronous oscillations with different phase shifts between the oscillations of the subsystems. At $p = 1$ stable limit cycle C_N represents the complete synchronization, i.e., $x_1 = x_2, y_1 = y_2, z_1 = z_2$. The antiphase synchronization (phase difference equals to π) is manifested by the saddle limit cycle C_S . Saddle cycles C_R and C_P represent the phase synchronization of subsystems with the phase difference between the interval $[0, \pi)$ -cycle C_R and $(\pi, 2\pi]$ -cycle C_P . Cycles C_P and C_R are symmetrical in the relation to cycle C_S as can be seen in Fig. 2(b).

The computation of the eigenvalues of fixed point P_R shows that it is a saddle (saddle-focus), in which two pairs of complex-conjugate eigenvalues have positive real parts and two other eigenvalues are real and negative. The analysis of the Floque multipliers of the limit cycles shows that the

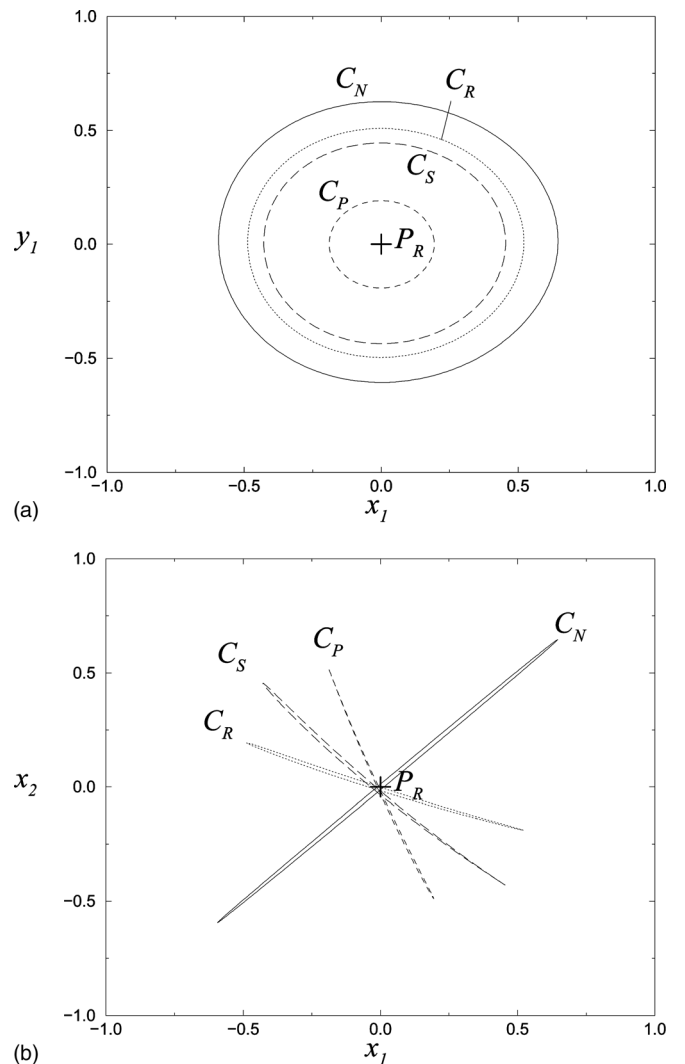


FIG. 2. Projections of the phase portrait of the trajectories of system (1); $m_1 = m_2 = 0.1, g = 0.2, \epsilon = 0.025, p = 1.001$: (a) on the plane $(y_1 - x_1)$, (b) on the plane $(x_2 - x_1)$. In phase space there are unstable fixed point P_R , saddle limit cycles C_S, C_P, C_R and stable limit cycle C_N .

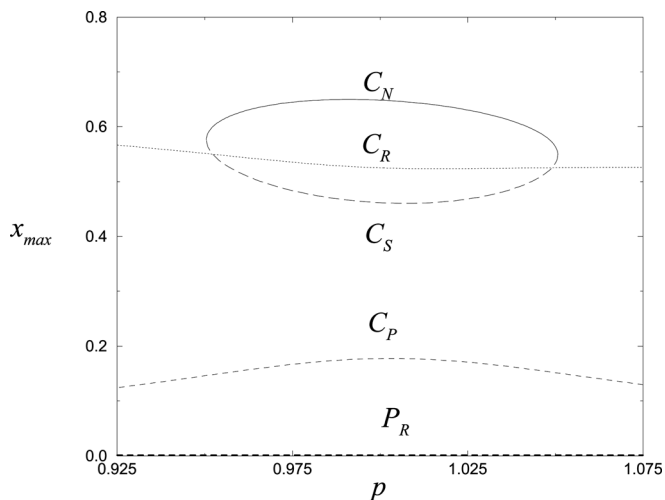


FIG. 3. Bifurcation diagram of the fixed point P_R and limit cycle C_N , for different values of the coefficient p : $m_1 = m_2 = 0.1$, $g = 0.2$, $\epsilon = 0.025$.

cycles C_P and C_R have three-dimensional stable and unstable manifolds. The cycle C_S passes four-dimensional stable and two-dimensional unstable manifolds. Cycles C_N and C_S are resonance ones and lie on the two-dimensional torus. Let us follow the bifurcations of these limit cycles and fixed point P_R on the plane of parameters $(\epsilon - p)$.

Figure 3 shows the bifurcation diagram for the limit cycles and the fixed point, depending on the detuning between frequencies p for a fixed value of coupling coefficient $\epsilon = 0.025$. In this diagram on the vertical axis the maximum values of dynamic variable $x_1 = x_{max}$ for the limit cycles and the fixed point (for the fixed point P_R the dynamic variable is zero) are shown. In the middle of the synchronization interval the stable cycle of C_N and the saddle cycle C_S have two pairs of complex conjugate multipliers with modula less than one, and two real multipliers, respectively, smaller and larger than one. The saddle cycles of C_R and C_P have pairs of real multipliers larger than one, pairs of complex-conjugate multipliers with modula smaller than one and single real multiplier smaller than one. When leaving area A as the result of the change of detuning parameter p , the bifurcations of the synchronous mode take place on the lines l_{SN} and l'_{SN} . Located on the torus the stable limit cycle C_N and the saddle cycle C_S approach each other when the control parameter p to bifurcation approaches lines l_{SN} and l'_{SN} . On these lines they merge together, one real multiplier of each cycle equals to +1 and after the point of bifurcation (in the region C of Fig. 1) they vanish and in the phase space there exists a stable two-dimensional ergodic torus. The phase trajectories on it are never closed. On this torus we observe quasiperiodic oscillations with two incommensurate frequencies. With further increase of the control detuning parameter p the saddle cycles C_R , C_P , and the fixed point P_R go out of the synchronization region A. At this exit they do not undergo any bifurcations and continue to have three-dimensional stable and three-dimensional unstable manifolds. Thus, in the region of the quasiperiodic oscillations of the C the phase portrait of system (1) consists of the stable ergodic torus, the saddle limit cycles C_R , C_P , and the unstable fixed point of P_R (located in the origin).

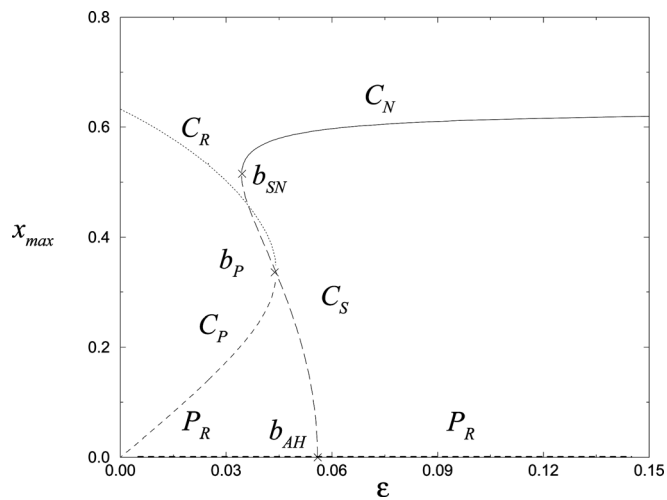


FIG. 4. Bifurcation diagram of the fixed point P_R and limit cycles C_P , C_N , C_S and C_R for different values of the coupling coefficient ϵ : $m_1 = m_2 = 0.1$, $g = 0.2$, $p = 1.034$.

Now let us consider what happens with the increase of the coupling coefficient ϵ . We fix $m = 0.1$, $p = 1.034$, and follow the bifurcations of the above mentioned limit sets. The bifurcation diagram is shown in Fig. 4. In the case of the weak coupling in the phase space, there exist the stable torus, the saddle cycles C_P and C_R , the unstable fixed point P_R . With an increase of ϵ when crossing line l_{SN} (see Fig. 1), the stable limit cycle of C_N and the saddle cycle of C_S are born on the torus. At the bifurcation diagram (Fig. 4), this corresponds to the point b_{SN} , from which two branches originate. The solid line is formed by the values of the dynamical variable on stable cycle of C_N , and the broken line by the values of this variable on the saddle cycle C_S . With further increase of the coupling coefficient the subcritical pitchfork bifurcation takes place on the line l_{SR} in the parameter plane $(\epsilon - p)$ (Fig. 1). The saddle cycles C_P and C_R approach the saddle cycle C_S and merge into it on the line l_{SR} . Above the point of this bifurcation a saddle limit cycle C_S remains, but has stable and unstable manifolds of a different character. The analysis of multipliers of these cycles shows that up to the bifurcation point saddle cycles C_P and C_R have three-dimensional stable manifolds and three-dimensional unstable manifolds, and the saddle cycle C_S four-dimensional stable and two-dimensional unstable manifolds which are enclosed by a stable limit cycle, forming a two-dimensional torus. After the point of the subcritical pitchfork bifurcation the saddle limit cycle C_S has three-dimensional stable and unstable manifolds. This leads to the destruction of two-dimensional torus, on which the resonant cycles are located. At the bifurcation diagram of Fig. 4 the pitchfork bifurcation is denoted by b_p . For the values of the coupling coefficient from the region bounded by the lines l_{SR} and l_{2H} in the $(\epsilon - p)$ parameter plane of Fig. 1, the phase portrait of the system (1) consists of an unstable fixed point P_R , the saddle limit cycle C_S , and the stable limit cycle C_N . Above the line l_{SR} two-dimensional torus does not exist anymore; it is destroyed in a subcritical pitchfork bifurcation of a saddle limit cycle C_S .

This bifurcation is connected with the transition from the phase locking region A to the region B inside the main

synchronization tongue $S_{1:1}$ (see Fig. 1). With further increase of ϵ the radius of saddle limit cycle C_S decreases. On the line l_{2H} it shrinks to the unstable fixed point P_R and we observe Andronov-Hopf bifurcation. Before the bifurcation the fixed point P_R has two pairs of complex conjugate eigenvalues with positive real parts and two real negative eigenvalues. After the bifurcation the point has a pair of complex eigenvalues with positive real parts and a pair of such eigenvalues with negative real parts, two real eigenvalues remain negative and equal to -0.2 .

For the strong coupling coefficient ϵ , above the line l_{2H} in synchronization region B of Fig. 1, in the phase space the stable limit cycle C_N and the unstable fixed point P_R exist. In this case the increase of the detuning parameter p leads to the amplitude death effect. As the detuning between characteristic frequencies $p = \omega_1/\omega_2$ increases, the amplitude of oscillations in each of the generators decreases to zero. Figure 5 shows the bifurcation diagram for the limit cycle C_N and the fixed point P_R for different values of the detuning parameter p and the fixed values of $m_1 = m_2 = 0.1$, $g = 0.2$, and $\epsilon = 0.125$. When the natural oscillations frequencies of the partial oscillators are equal ($p = 1$) the radius of a stable limit cycle C_N , corresponding to the synchronization regime has a maximum value. With the increase or decrease of the detuning parameter p this radius smoothly decreases, cycle C_N shrinks to the fixed point P_R at the origin. At the transition from the region B to the region D the fixed point P_R undergoes bifurcation from an unstable saddle-focus in the stable focus so we have a supercritical Andronov-Hopf bifurcation. In the region D , system (1) has only one attractor in the phase space: a stable fixed point P_R . The self-oscillations are absent as the coupling results in their suppression, despite the fact that each of the subsystems is in an excited state for $\epsilon = 0$.

At the transition from region D to region B (Fig. 1) (e.g., at a fixed coupling coefficient ϵ and changing detuning parameter p), periodic oscillations are smoothly excited. However, at the transition from region D into region C , with the decrease in the coupling ϵ and fixed detuning p , one observes soft excitation of the quasi-periodic oscillations. The bifurca-

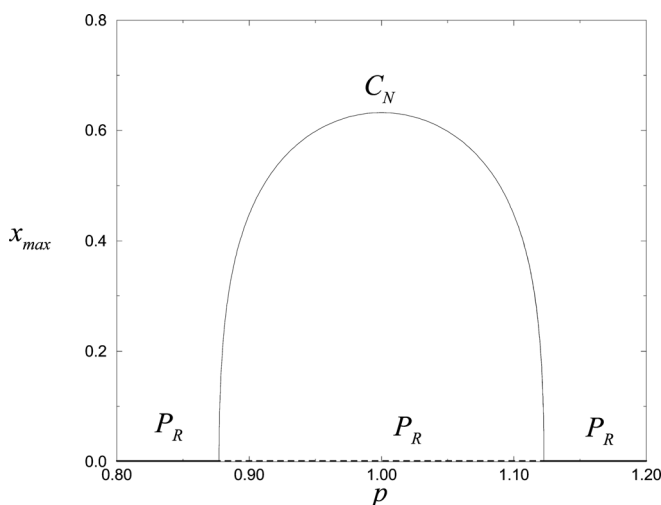


FIG. 5. Bifurcation diagram of the fixed point P_R and limit cycle C_N , for different values of the coefficient p : $m_1 = m_2 = 0.1$, $g = 0.2$, $\epsilon = 0.125$.

tional lines l_H and l'_H define the boundaries between the regions of amplitude death and quasiperiodic oscillations.

In region D , up to the lines l_H and l'_H , the fixed point P_R has two pairs of complex-conjugate eigenvalues with negative real parts and two real negative eigenvalues. On the lines l_H and l'_H the real parts of the complex conjugate eigenvalues vanish (two pairs of purely imaginary eigenvalue), and below these lines are positive. This results in the smooth birth of the attracting torus T and saddle cycles of C_P and C_R in the vicinity of the fixed point P_R . With the decrease of the coupling coefficient ϵ , these limit sets (the fixed point, two saddle limit cycles, and the attracting torus) diverge from each other.

The described bifurcation of the birth of the attracting torus and the two saddle cycles from a fixed-point is degenerated due to the identity of the partial oscillators (the excitation parameters m_1 and m_2 are equal). The identity of the control parameters in the uncoupled generators results not only in this degenerate situation but also in the pitchfork bifurcation, which occurs on line l_{SR} in the main synchronization tongue $S_{1:1}$ (Fig. 1) and which involves saddle cycles C_S , C_P , C_R (see bifurcation diagram in Fig. 4). The introduction of non-identity oscillators in the parameters $m_{1,2}$ eliminates this degeneracy and results in the typical bifurcation transitions.

B. The effect of the additional mismatch of the excitation parameters ($m_1 \neq m_2$) on the bifurcation mechanism of the synchronization and the amplitude death

We consider the dynamics of the weakly non-identical generators in the neighborhood of the main synchronization tongue $S_{1:1}$ in more details. Figure 6 presents the bifurcation diagram of the system (1) on the plane of control parameters ($\epsilon - p$) for the weakly non-identical oscillators ($m_1 = 0.105$, $m_2 = 0.1$). Here, as in the identical case, the synchronization regions are denoted by A and B , the region of quasi-periodic oscillations by C and the region of the amplitude death by D . It is evident that the weak nonidentity of the subsystems

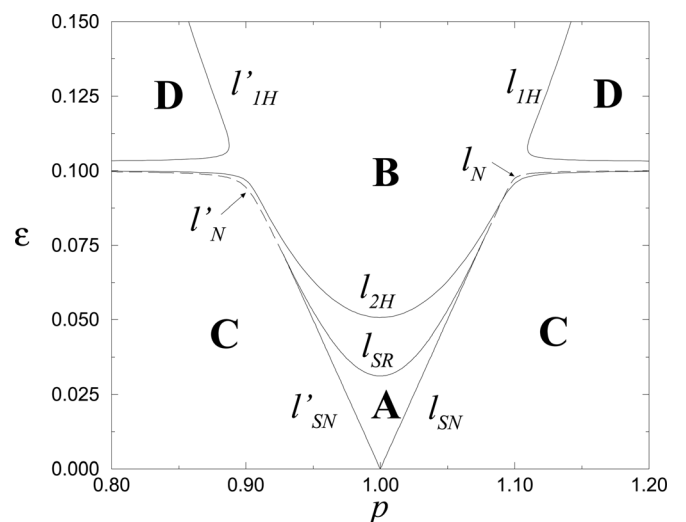


FIG. 6. Bifurcation diagram of the system (1) in the main area of synchronization region $S_{1:1}$ on the plane of control parameters ($\epsilon - p$), (coupling coefficient, detuning parameter): $m_1 = 0.105$, $m_2 = 0.1$, $g = 0.2$.

leads to a significant change in the structure of the parameter space. On the boundary between areas *C* and *D*, a narrow channel in which there exists a stable limit cycle corresponding to the regime of the synchronization appear. This channel exists for a wide range of detuning parameter p .

The appearance of this channel makes a qualitative change in the structure of the bifurcation transitions. Let us analyze this change in details. In region *A* the phase portrait of system (1) is the same as in the previous case of identical subsystems (Fig. 2). It consists of an unstable fixed point P_R , the saddle cycles C_P, C_R , and the resonant cycles on the torus T , i.e., a saddle cycle C_S and a stable cycle C_N . For the decreasing values of ϵ the exit from the synchronization region occurs on the lines l_{SN} and l'_{SN} through the saddle-node bifurcation of the limit cycles C_N and C_S . The phase portraits and the sequences of bifurcations are the same as in the identical subsystems case.

The changes in the structure of the parameter space are observed for larger values of ϵ . Figure 7 shows the bifurcation diagram of the limit cycles and the fixed point for the increasing values of ϵ and the low fixed value of frequency detuning ($p = 1.034$). For the weak coupling, left point b_{SN} (in Fig. 6 below the line l_{SN}), in the phase space an unstable fixed point P_R , two saddle limit cycles C_P, C_R , and the stable two-dimensional torus T exist. With the increase of the coupling, the bifurcation takes place in the point b_{SN} and a pair of limit cycles C_N and C_S is born on the torus T . With further increase of coupling parameter ϵ the saddle limit cycle C_S with two-dimensional unstable and four-dimensional stable manifolds approach the other saddle limit cycle C_R characterized by three-dimensional stable and unstable manifolds. At the point b_{SR} they merge together and disappear. This leads to the destruction of torus T , on which the resonance limit cycles, stable C_N and saddle C_S , have been located. As can be seen in Fig. 7 with an increase of the coupling, a saddle limit cycle C_P initially increases in size and then gradually decreases. At the point b_{AH} it undergoes Andronov-Hopf bifurcation. Fixed point P_R changes its stability from an unstable saddle-focus with two pairs of complex conjugate

eigenvalues with positive real parts to unstable saddle-focus, which has one pair of complex conjugate eigenvalue with negative real and one pair with positive real parts. (Two remaining real and negative eigenvalues do not change at this bifurcation). In the synchronization region *B* in the phase space an unstable fixed point P_R and the stable limit cycle C_N exist. Thus, a small additional mismatch of the parameters $m_{1,2}$ results in the elimination of the pitchfork bifurcation. Now the destruction of the torus during the transition from the synchronization region *A* to the synchronizations region *B* occurs as the result of saddle-saddle bifurcations of two limit cycles C_S and C_R .

Figure 8 shows another bifurcation diagram of the limit cycles C_R, C_P, C_N , and fixed point P_R for larger detuning ($p = 1.12$). It describes the bifurcations leading to effect of the amplitude death at the transition, from the region of quasi-periodic oscillations *C* to the region of the amplitude death *D*. For the weak coupling in the phase space a two-dimensional attracting torus T , the saddle limit cycles C_P, C_R , and unstable fixed point P_R (at the origin) exist. With the increase of ϵ , the radius of the saddle limit cycle C_P initially increases. Then it decreases and shrinks to the fixed point P_R . At the point b_{2H} Andronov-Hopf bifurcation is observed which in the parameters plane ($\epsilon - p$) corresponds to the bifurcation line l_{2H} (see Fig. 6). After this bifurcation the fixed point P_R has a pair of complex conjugate eigenvalues with a positive real parts, a pair of such eigenvalues with negative real part and two real negative eigenvalues. At the same time with the increase of ϵ the size of a saddle limit cycle C_R decreases, and after point b_N in the bifurcation diagram of Fig. 8 it turns from the saddle to the stable limit cycle. This corresponds to the Neimark-Sacker bifurcation. The stable two-dimensional torus contracts to a saddle limit cycle C_R which after the bifurcation becomes stable. In Fig. 6 this bifurcation occurs on l_N on which quasiperiodic oscillations are replaced by periodic oscillations. With further increase of the coupling, the radius of a stable limit cycle decreases to zero and the cycle C_R is contracted to the

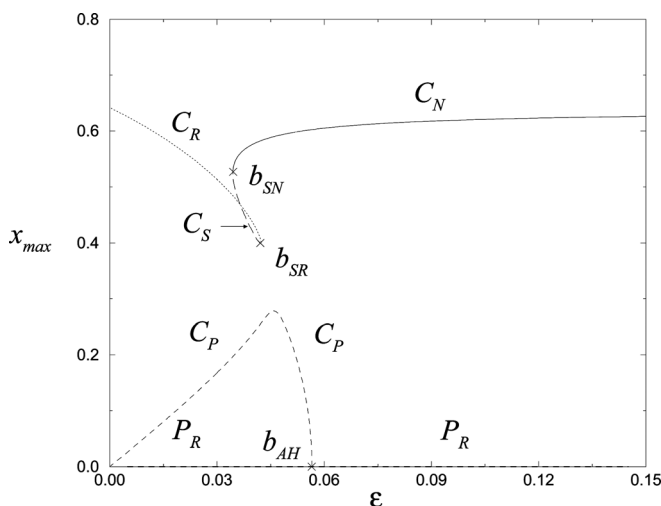


FIG. 7. Bifurcation diagram of the fixed point P_R and limit cycles C_P, C_N, C_S and C_R for different values of the coupling coefficient ϵ , and additional mismatch: $m_1 = 0.105, m_2 = 0.1, g = 0.2, p = 1.034$.

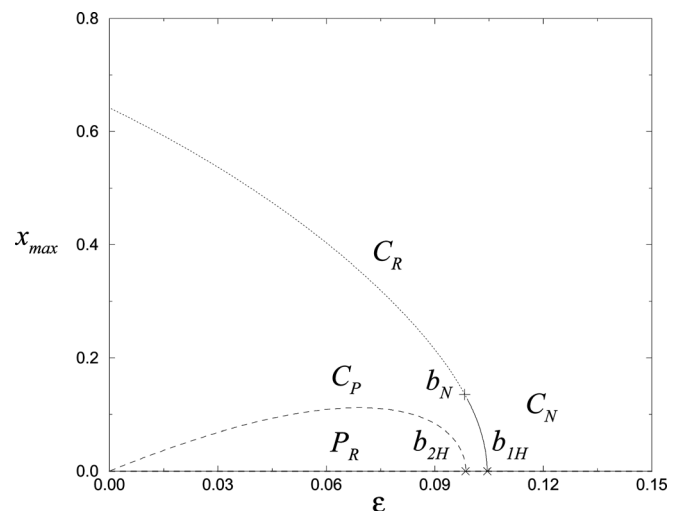


FIG. 8. Bifurcation diagram of the fixed point P_R and limit cycles C_P, C_N, C_S and C_R for different values of the coupling coefficient ϵ , and additional mismatch: $m_1 = 0.105, m_2 = 0.1, g = 0.2, p = 1.12$.

unstable fixed point P_R , in the Andronov-Hopf bifurcation (point b_{1H} in Fig. 8). After this the fixed point becomes stable in system (1) and the complete suppression of self-oscillations is observed.

IV. THE BIFURCATION ANALYSIS OF THE OSCILLATORY REGIMES IN A NEIGHBORHOOD OF SYNCHRONIZATION MODE $n : m$

In Sec. III we have analyzed the bifurcations which occur in the main area of synchronization $S_{1:1}$ and its neighborhood for different values of coupling and detuning parameters (ϵ and p , respectively). In this section we investigate the bifurcations which occur in other synchronization regions.

A. The case of two oscillators with identical excitation parameters $m_1 = m_2$

Figure 9 shows the synchronization tongue of system (1) with different values of rotation numbers which are located on the right side of the main synchronization region $S_{1:1}$. Both subsystems are identical $m_1 = m_2 = 0.1$ and $g = 0.2$ and in the lack of coupling ($\epsilon = 0$) are characterized by quasi-harmonic oscillations. It is evident that in comparison with the main synchronization tongue ($S_{1:1}$) the additional synchronization tongues $S_{1:2}, S_{1:3}, S_{2:3}, S_{3:4}$ are considerably narrower and limited at the top by the amplitude death region D . They start at the line $\epsilon = 0$ and terminate on the line l''_H . Both at the bottom and at the top they converge to a single point. According to their bifurcation structure these tongues are qualitatively different. In regions $S_{2:3}$ and $S_{3:4}$ one can observe the synchronization at saddle-node bifurcation while in tongues $S_{1:2}$ and $S_{1:3}$ two synchronization regions (A and B) are present. Figures 10(a) and 10(b) show in larger scale the synchronization tongues $S_{1:2}$ and $S_{2:3}$, respectively. The synchronization tongue $S_{1:2}$ has $A_{1:2}$ and $B_{1:2}$ regions. The region $A_{1:2}$ is bounded by the lines of saddle-node bifurcation l_{SN}, l'_{SN} and l_{SR} . The region $B_{1:2}$ is bounded by the line

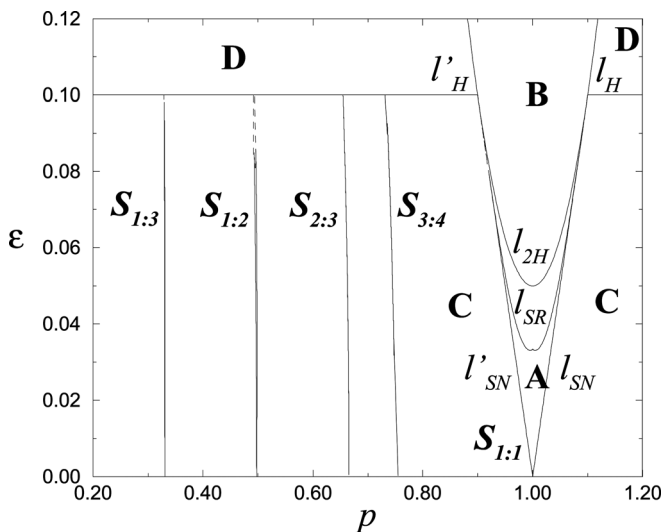


FIG. 9. Synchronization regions with different rotation numbers $S_{1:1}, S_{1:2}, S_{1:3}, S_{2:3}, S_{3:4}$ and the amplitude death region D on the plane of system (1) parameters ($\epsilon - p$): $m_1 = m_2 = 0.1, g = 0.2$.

of saddle-node bifurcation l_{SR} and the lines Neimark-Sacker bifurcation l_{SN} and l'_{SN} . With the decrease of coupling, the lines of saddle-node bifurcations l_{SN} and l'_{SN} join each other on the axis $\epsilon = 0$. With an increase of the coupling, the lines of Neimark-Sacker bifurcation l'_N, l_N converge to the same point on the line l'_H which bounds the region of the amplitude death D . The synchronization tongue $S_{2:3}$ has only synchronization region $A_{2:3}$, which is bounded by the lines of saddle-node bifurcation l_{SN} and l'_{SN} . Both with the decrease and increase of coupling, these lines converge to the points on the line $\epsilon = 0$ and l'_H , respectively.

Figure 11 shows the projections of phase portraits in the regions $A_{1:2}$ and $A_{2:3}$. In both cases, the phase portrait consists of the unstable fixed point P_R , saddle limit cycles C_P and C_R , as well as the resonant limit cycles C_S and C_N , located on two-dimensional torus T .

The limit cycle C_N is stable and represents the synchronization regime. The saddle limit cycle C_S has a two-dimensional unstable manifold on which the stable limit cycle C_N is locked and four-dimensional stable manifold. The stability types and the periods of the saddle limit cycles C_P and C_R

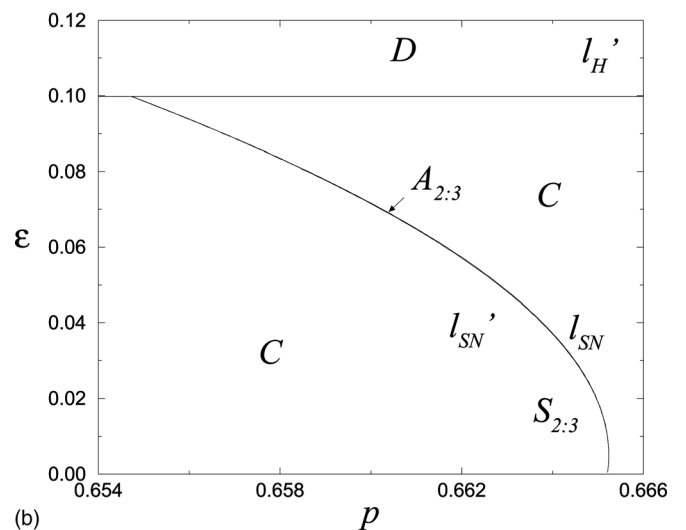
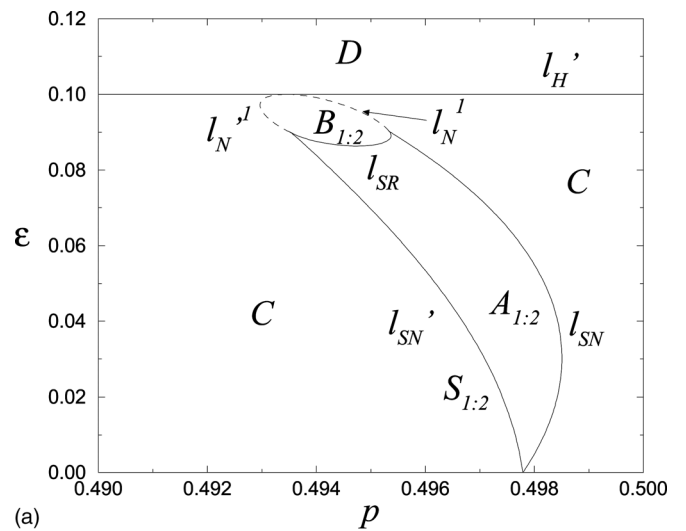


FIG. 10. Synchronization tongues of the system (1): $m_1 = m_2 = 0.1, g = 0.2$. (a) Tongue $S_{1:2}$, containing the region $A_{1:2}$ and the region $B_{1:2}$; (b) tongue $S_{2:3}$ containing only region $A_{2:3}$.

are the same for the wide range of coupling coefficient ϵ in all synchronization tongues. With the change of the detuning parameter p , these saddle cycles do not undergo any bifurcations. The resonance limit cycles on the torus C_N and C_S exist only in the phase locked synchronization tongues and in different tongues have different periods [see Figs. 11(a) and 11(b)]. When changing the detuning parameter p they disappear.

Let us examine the changes of the phase portraits presented in Figs. 11(a) and 11(b) which occur with the increase of the coupling coefficient ϵ and the fixed values of other parameters. Figure 12(a) presents the bifurcation diagram for the fixed point P_H and limit cycles $C_S, C_N, C_P,$ and C_R for different values of ϵ in the synchronization tongue $S_{1:2}$ ($p = 0.495$). In Figure 12(b) the enlargement of the part of Figure 12(a) is shown.

At the weak coupling [in region C, below the line l'_{SN} on the parameter plane of Fig. 10(a)] in the phase space, an unstable fixed point P_R , the saddle limit cycles $C_P, C_R,$ and the stable two-dimensional torus corresponding to the regime

of quasi-periodic oscillations exist. The fixed point P_R has two real negative eigenvalues and two pairs of complex conjugate eigenvalues with positive real parts. The saddle limit cycles C_P and C_R have three-dimensional stable and unstable manifolds. The limit cycle C_P is born as the result of the Andronov-Hopf from the unstable fixed point P_R on the line $\epsilon = 0$. The saddle limit cycle C_R is surrounded by the attracting two-dimensional torus T . With the increase of the coupling, while crossing line l'_{SN} [Fig. 10(a)] a pair of resonant limit cycles: saddle C_S and stable C_N is born on the torus. On the bifurcation diagram in Figs. 12(a) and 12(b) the interval of coupling parameter ϵ , for which resonant cycles C_N and C_S exist, coincides with phase locked region $A_{1:2}$. With further increase of coupling the saddle-saddle bifurcation is observed. The limit cycle C_R with three-dimensional stable and unstable manifolds merges with the resonant limit cycle C_S characterized by two-dimensional unstable and four-dimensional stable manifolds. After the bifurcation point the resonant cycles disappear. There is a destruction of the torus, then in the phase space there exist a stable limit cycle C_N , the saddle limit cycle C_P , and an unstable fixed point P_R . In Fig. 10(a) this corresponds to the transition from region $A_{1:2}$

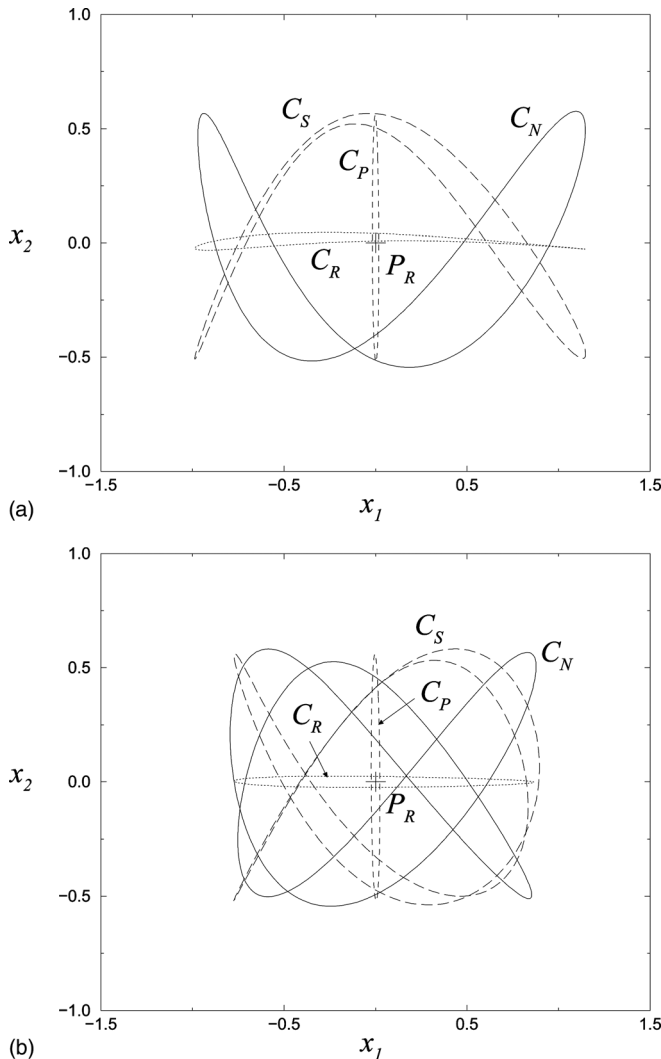


FIG. 11. Projections of the phase portraits of the trajectories of the system (1): $m_1 = m_2 = 0.1, g = 0.2$. (a) In the synchronization tongue $S_{1:2}$: $\epsilon = 0.025, p = 0.498$ (region $A_{1:2}$), (b) in the synchronization region $S_{2:3}$: $\epsilon = 0.025, p = 0.665$.

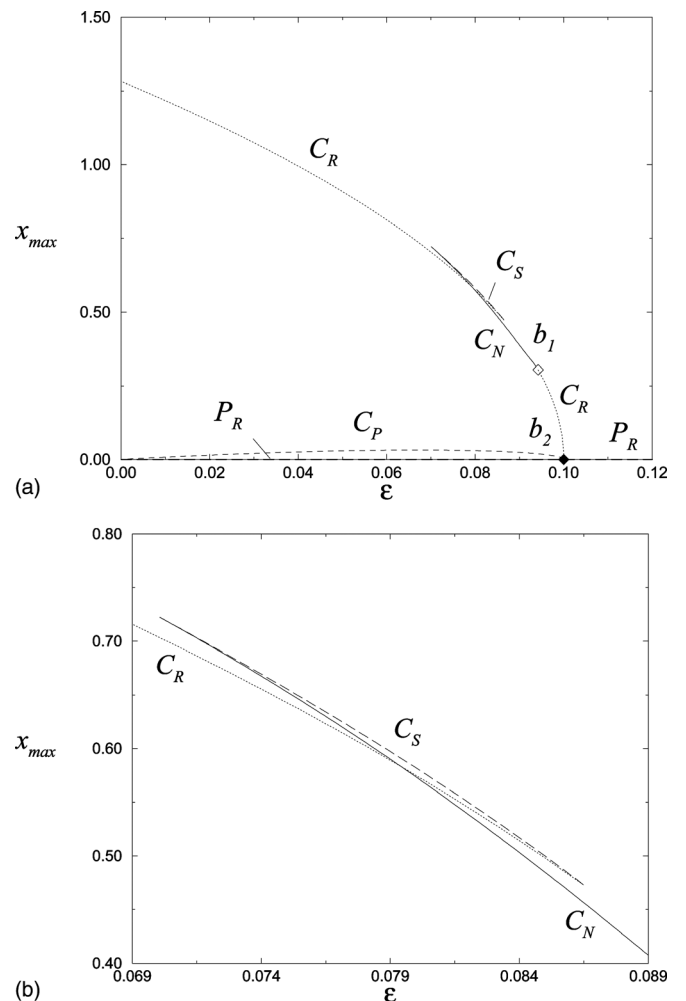


FIG. 12. (a) Bifurcation diagram of the fixed point P_R and limit cycles C_P, C_N, C_S and C_R for different values of the coupling coefficient ϵ : $m_1 = m_2 = 0.1, g = 0.2$ in the synchronization tongue $S_{1:2}$ ($p = 0.495$), (b) enlargement of (a).

to the synchronization region $B_{1:2}$. With further increase of the coupling parameter ϵ Neimark-Sacker bifurcation occurs [point b_1 in Fig. 10(a)], limit cycle C_N loses its stability and stable two-dimensional torus is born. This bifurcation corresponds to the transition from the synchronization tongue $S_{1:2}$ to the region of quasiperiodic oscillations. In the range of the values of coupling coefficient, bounded by the points b_1 and b_2 , in the phase space: the unstable fixed point P_R , the saddle limit cycles C_R, C_P and two-dimensional torus T exist. When approaching point b_2 (in the bifurcation diagram), torus T and limit cycles C_R, C_P shrink to a fixed point P_R . In this bifurcation fixed point P_R becomes stable. In Fig. 10(a) this bifurcation corresponds to the transition to the region D (amplitude death). The described bifurcation, when the torus and two cycles simultaneously converge into a fixed point is possible due to the identity of excitation parameters $m_1 = m_2$ and inertial parameters $g_1 = g_2$ in both subsystems.

Changing the coupling coefficient ϵ inside the synchronization tongue $S_{2:3}$, one observes simple transformations of the phase portraits [Fig. 11(b)]. For any value of p in the neighborhood of $S_{2:3}$ [see Fig. 10(b)] the phase portrait consists of the unstable fixed point P_R , the saddle limit cycles C_P, C_R , and the attractive two-dimensional ergodic torus T which corresponds to the regime of quasi-periodic oscillations. At the boundaries of tongue $S_{2:3}$ the saddle-node bifurcation of the resonant limit cycles C_S and C_N located on the torus T occurs. With the increase of coupling, when crossing line l'_H the degenerate bifurcation occurs—the saddle cycles C_P, C_R , and stable two-dimensional torus T shrink to fixed point P_R . P_R becomes stable and the amplitude death is observed in system (1).

Thus, for the case of identical excitation ($m_1 = m_2$) and inertial ($g_1 = g_2$) parameters of the interacting oscillators one can observe the synchronization tongues with different rotation numbers and region of the amplitude death on the plane of the considered control parameters, i.e., the coupling coefficient ϵ versus the detuning of the natural frequencies p . The synchronization tongues with the rotation numbers different from 1:1 are limited to the given intervals of the coupling coefficient ϵ . Their boundaries converge to a single point not only on the axis $\epsilon = 0$, but also on the boundary l'_H , representing the boundary of the amplitude death region D . The synchronization tongues can be divided into two groups. Some of them contain both A and B synchronization regions, while others only the A regions.

B. The effect of the asymmetry of subsystems on the transitions to synchronization regimes

Now we consider how the bifurcation structure is changed in the case of different excitation parameters in both subsystems, i.e., $m_1 \neq m_2$. Weak non-identity of excitation parameters m_1 and m_2 leads to the significant changes in the structure of bifurcations in the neighborhood of the boundary of the amplitude death region D . The results presented in Fig. 13 have been calculated for the same values of the control parameters as the results of Fig. 9, except the small additional mismatch 0.005 in the excitation parameters ($m_1 = 0.105, m_2 = 0.1, g_1 = g_2 = 0.2$). One can notice that the weak

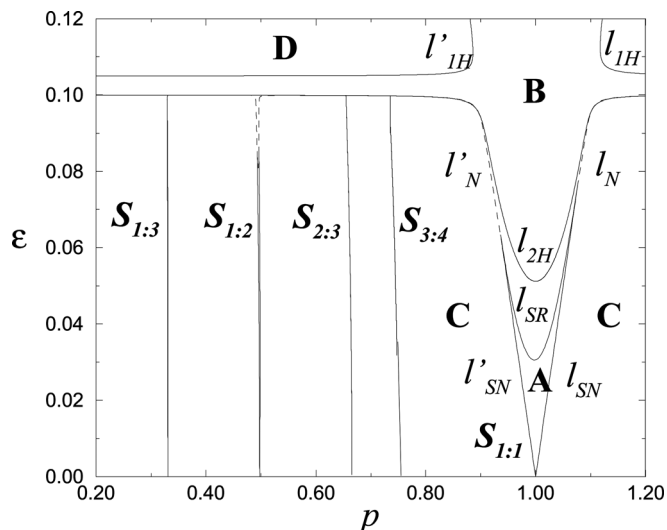


FIG. 13. Synchronization regions with different rotation numbers $S_{1:1}, S_{1:2}, S_{1:3}, S_{2:3}, S_{3:4}$ and the amplitude death region D on the plane of system (1) parameters ($\epsilon - p$): $m_1 = 0.105, m_2 = 0.1, g = 0.2$

nonidentity leads to the splitting of the boundary of the region D . Instead of one line l'_H (as in Fig. 9) three bifurcation lines are observed (Fig. 13), namely, l'_{IH} —line of the bifurcation in which a stable limit cycle C_N is born out of the stable fixed point P_R ; l_{2H} —the birth of saddle limit cycle C_P out of unstable fixed point P_R ; l'_N —two-dimensional stable torus T is born out of the stable limit cycle C_N . As the result of the described boundary splitting a channel that separates the region of quasi-periodic oscillations C and region of amplitude death D , in which there exists a stable limit cycle C_N has been created. Inside the channel the limit cycle C_N does not undergo any bifurcations.

In the previous case, of equal values m_1 and m_2 (Fig. 9) the boundaries of the synchronization tongues converge to a point both for the decrease and increase of the coupling parameter. All of the synchronization tongues have been closed and transitions between synchronous oscillations with different rotation numbers occur only through the bifurcation of the appropriate stable limit cycles.

For weak non-identity of m_1 and m_2 (Fig. 13), the synchronization tongues $S_{2:3}$ and $S_{3:4}$, consisting only of the phase locked synchronization region, remain closed. With the increase of coupling their boundaries converge to a point on line l'_n (the birth of torus bifurcation). At the same time, the synchronization tongues $S_{1:1}, S_{1:2}, S_{1:3}$, consisting of A and B synchronization regions merge together and become open. With an increase of coupling their upper boundaries do not converge to a single point. As a result, a stable limit cycle C_N can be “transferred” from the phase locking synchronization region of one of the open synchronization tongues to the phase locking region of another open synchronization tongue, without undergoing any bifurcation. The transitions between the synchronization tongues with different rotation numbers can be achieved without any bifurcation in a smooth evolutionary manner.

Figure 14 shows the open $S_{1:2}$ and the closed $S_{2:3}$ synchronization tongues. The phase portraits in the phase locking synchronization regions $A_{1:2}, A_{2:3}$ are qualitatively the

same as in the case of identical ones presented in Fig. 11. Let us investigate the transformation of phase portraits, depending on the changes of the coefficient of coupling ϵ (with fixed value of detuning parameter p) inside the synchronization tongues $S_{1:2}$ and $S_{2:3}$.

The boundaries of $S_{2:3}$ consist of a line of saddle-node bifurcations which with the increase of coupling converge to a point on line l'_N of the birth of the torus T , i.e., there is always a saddle-node bifurcation to the torus T in which the resonance limit cycles C_N and C_S [Fig. 11(b)] merge and disappear. With the increase of ϵ , two-dimensional torus T decreases and shrinks to the saddle limit cycle C_R , which above the line l'_N becomes stable. Simultaneously another saddle limit cycle C_P decreases and on the line l_{2H} shrinks to unstable fixed point P_R . This corresponds to Andronov-Hopf bifurcation, after which the saddle fixed point with four-dimensional unstable manifold transforms to a saddle fixed point with two-dimensional unstable manifold (one pair of complex-conjugate eigenvalues with positive real parts). As the result of this, in the channel separating the region of

quasi-periodic oscillations C and the region of amplitude death D , the phase portrait consists of the stable limit cycle and the unstable fixed point of the form of a saddle-focus. With further increase of the coupling coefficient ϵ , a stable limit cycle shrinks to a fixed point on the line l'_{IH} where Andronov-Hopf bifurcation occurs. After this bifurcation fixed point, P_R becomes stable and self-oscillations vanish.

Let us investigate the transformation of phase portraits inside the phase locking synchronization region $A_{1:2}$ [Fig. 11(a)]. Figure 15 presents the bifurcation diagrams for the fixed point P_R , the limit cycles C_P , C_R , C_S , and C_N in the synchronization tongue $S_{1:2}$, and in its neighborhood.

For $p = 0.496$ [Fig. 15(a)] and weak coupling ($0 < \epsilon \leq 0.05$) in the phase space, an unstable fixed point P_R , the saddle limit cycle C_P , and the saddle limit cycle C_R which is surrounded by two-dimensional stable torus T exist. In the system (1) the quasi-periodic oscillations are observed. With the increase of coupling ϵ at the entrance to the phase locking synchronization region, a saddle-node bifurcation is observed on the torus T and the resonant cycles C_N (stable) and C_S (saddle) are born. Next, the transition from the region A to the synchronization region B occurs as the result of the

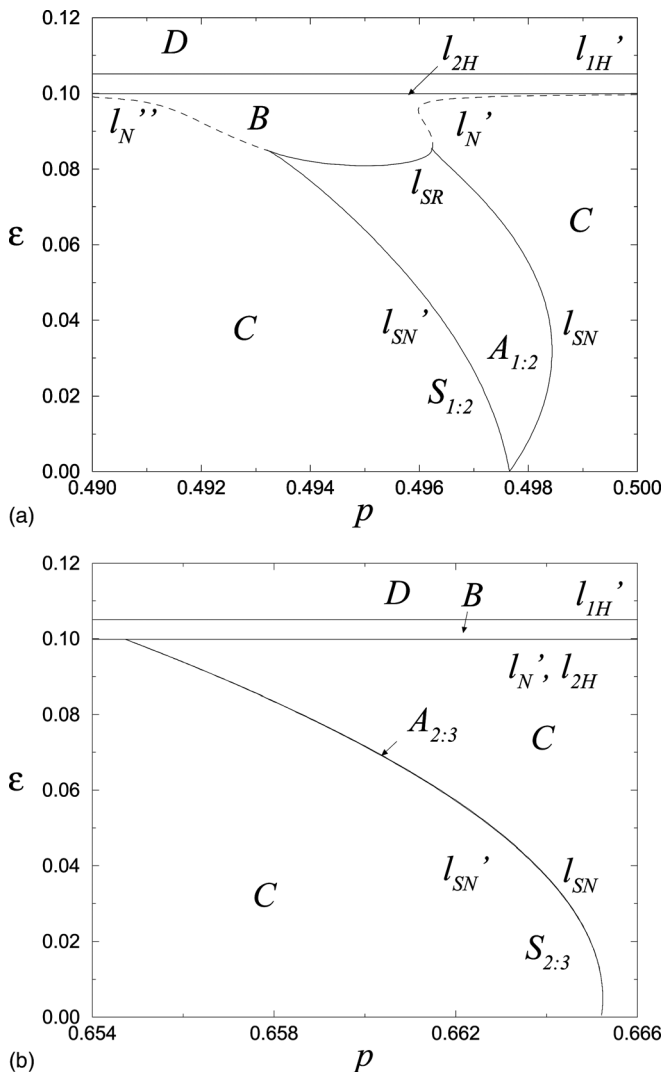


FIG. 14. Synchronization tongues of the system (1) with additional mismatch $m_1 = 0.105$, $m_2 = 0.1$, $g = 0.2$: (a) tongue $S_{1:2}$, containing the region $A_{1:2}$ and the region $B_{1:2}$, (b) tongue $S_{2:3}$ containing region $A_{2:3}$.

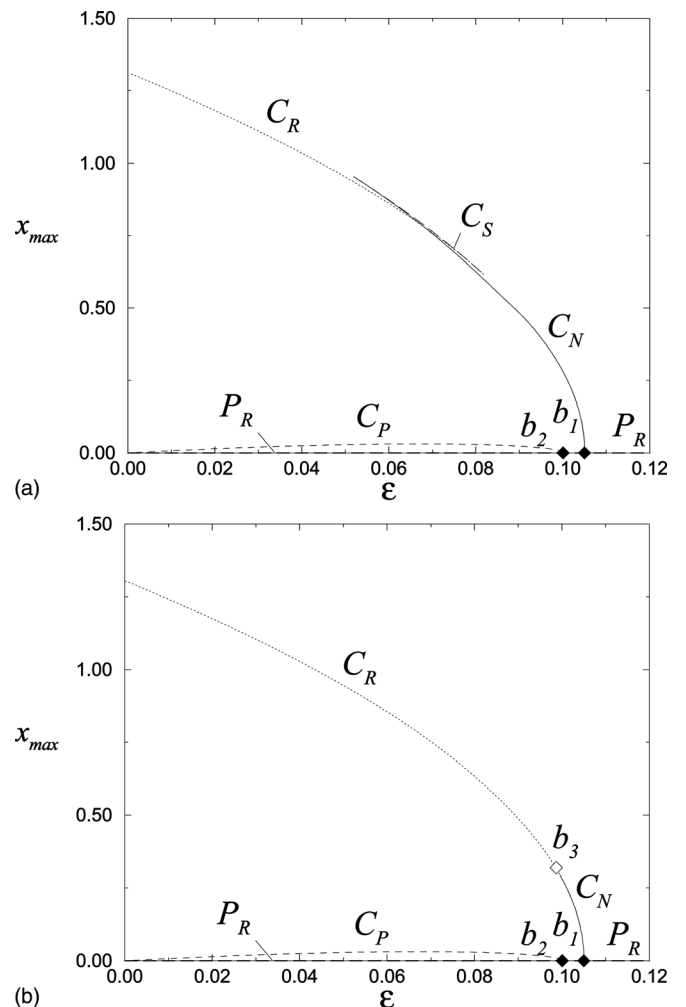


FIG. 15. Bifurcation diagrams of the fixed point P_R and limit cycles C_P , C_N , C_S , and C_R for different values of the coupling coefficient ϵ : $m_1 = 0.105$, $m_2 = 0.1$, $g = 0.2$; (a) in the synchronization tongue $S_{1:2}$ ($p = 0.496$), (b) right of the tongue $S_{1:2}$ ($p = 0.499$).

destruction of two-dimensional torus in the bifurcation, in which the resonant saddle limit cycles C_S and C_R merge together and disappear. The stable limit cycle C_N does not undergo any bifurcation, i.e., with an increase of coupling ϵ the synchronization state continues to occur in the channel separating the region of quasi-periodic oscillations C and the region amplitude death D .

In the neighborhood of tongue $S_{1:2}$ for $p=0.499$ with the variation of the coupling parameter, saddle-node bifurcations on the torus are not observed. With the increase of ϵ , a stable limit cycle C_N is observed in the synchronization region of system (1). There is a transition from quasi-periodic to periodic oscillations, but it happens as a result of secondary Andronov-Hopf (or Neimark-Sacker) bifurcation. With further increase of coupling when approaching point b_3 on the bifurcation diagram of Fig. 15(b), the attracting two-dimensional torus shrinks to a saddle cycle C_R . Beyond point b_3 the torus disappears and the unstable limit cycle C_R becomes stable and the synchronization region B appears. With further increase of coupling ϵ (when the crossing point b_1), the stable limit cycle C_N shrinks to the fixed point P_R which turns into a stable one. Thus, we observe the transition from the region of periodic oscillations to the region of amplitude death.

The introduction of a small additional mismatch of the excitation parameters m_1 and m_2 in partial oscillators induces a qualitative change in the structure of the bifurcation set. On the plane of parameters the line of the degenerate bifurcation from the stable fixed point to the stable two-dimensional torus splits into three lines (two Andronov-Hopf bifurcations, and one Neimark-Sacker bifurcation). As the result, the channel that separates the region of the stable torus (ergodic or resonance) and the region of the stable fixed point is created. There is a stable limit cycle. At this transformation of the structure, the bifurcation set synchronization tongues $S_{1:1}$, $S_{1:2}$, $S_{1:3}$ merge.

V. CONCLUSIONS

The paper describes the dynamics of two dissipatively coupled generators with the inertial nonlinearity. We investigate the bifurcation transitions in the regimes of synchronization and the amplitude death. In the plane of control parameters we calculated the corresponding lines of the bifurcations for the cases of identical and weakly non-identical subsystems.

We identify the bifurcation set which creates the infinitely long band between the regions of amplitude death and quasi-periodic behavior, the so-called broadband synchronization.¹⁸ Additionally, it is shown that the synchronization tongues can be of two types: in one type there exist two (A and B) synchronization regions, while in the second one only the phase locking synchronization region exists. For weak non-identity of the excitation parameters the first type of tongues and the existence of the infinitely long band between the regions of amplitude death and quasiperiodic behavior allow the possibility of transition from one synchronization tongue to another one without bifurcation of a stable limit cycle, i.e., the transitions between the synchronized

tongues with different rotation numbers can proceed in an evolutionary manner. This is due to the fact that the Neimark-Sacker bifurcation lines which limit the synchronization tongues converge to the points and thus open and unify synchronization tongues $S_{1:1}$, $S_{1:2}$, $S_{1:3}$.

ACKNOWLEDGMENTS

V.A. and S.K. are indebted to the Technical University of Lodz for hospitality. T.K. acknowledges the support of the Foundation for Polish Science, Team Programme—Project No. TEAM/2010/5/5.

- ¹C. Huygens, "Letter to de Sluse," In: *Oeuvres Completes de Christian Huygens* (Letter Nos.: 1333 of 24 February 1665, 1335 of 26 February 1665, 1345 of 6 March 1665) (Societe Hollandaise Des Sciences, Martinus Nijhoff, La Haye, 1893).
- ²C. Huygens, *The Pendulum Clock* (Iowa State University Press, Ames, 1986). [*Horologium Oscillatorium* (Apud F. Muquet, Parisiis, 1673)].
- ³J. W. Strutt (Lord Rayleigh), *The Theory of Sound* (Macmillan and Co., Ltd., London, 1896), Vol. 2.
- ⁴I. I. Blekham, *Synchronization in Science and Technology* (ASME, New York, 1988).
- ⁵Y. Kuramoto, *Chemical Oscillations, Waves and Turbulence* (Springer, Berlin, 1984).
- ⁶Yu. M. Romanovsky, N. V. Stepanova, D. S. Chernavsky, *Mathematical Biophysics* (Nauka, Moscow, 1984) (in Russian).
- ⁷P. S. Landa, *Nonlinear Oscillations and Waves in Dynamical Systems* (Kluwer Academic Publishers, Dordrecht, Boston, London, 1996).
- ⁸A. Pikovsky, M. Resenblum, and J. Kurths, *Synchronization: An Universal Concept in Nonlinear Sciences* (Cambridge University Press, Cambridge, 2001).
- ⁹V. Anishchenko, V. Astakhov, A. Neiman, T. Vadivasova, and L. Shimansky-Geier, *Nonlinear Dynamics of Chaotic and Stochastic Systems* (Springer, Berlin, 2007).
- ¹⁰A. Balanov, N. Janson, D. Postnov, O. Sosnovtseva, *Synchronization. From Simple to Complex* (Springer, Berlin, 2009).
- ¹¹Y. A. Kuznetsov, *Elements of Applied Bifurcation Theory* (Springer, Berlin, 1998).
- ¹²D. G. Aronson, G. B. Ermentrout, and N. Kopell, *Physica D* **41**, 403 (1990).
- ¹³V. Kirk, *Physica D* **66**, 267 (1993).
- ¹⁴R. Mettin, U. Parlitz, and W. Lauterborn, *Int. J. Bifurcation Chaos* **3**, 1529 (1993).
- ¹⁵M. A. Taylor and I. G. Kevrekidis, *Physica D* **51**, 274 (1991).
- ¹⁶A. Algaba, M. Merino, and A. J. Rodriguez-Luis, *Int. J. Bifurcation Chaos* **11**, 513 (2001).
- ¹⁷A. P. Kuznetsov, N. V. Stankevich, and L. V. Turukina, *Physica D* **238**, 1203 (2009).
- ¹⁸A. P. Kuznetsov and J. P. Roman, *Physica D* **238**, 1499 (2009).
- ¹⁹M. V. Ivanchenko, G. V. Osipov, V. D. Shalfeev, and J. Kurths, *Physica D* **189**, 8 (2004).
- ²⁰A. G. Balanov, N. B. Janson, V. V. Astakhov, and P. V. E. McClintock, *Phys. Rev. E* **72**, 026214 (2005).
- ²¹K. Bar-Eli, *Physica D* **14**, 242 (1985).
- ²²M. A. Taylor and I. G. Kevrekidis, *Physica D* **51**, 274 (1991).
- ²³E. Doedel, R. C. Paffenroth, T. F. Fairgrieve, Y. A. Kuznetsov, B. E. Oldeman, B. Sandstede, and X. Wang, "AUTO-2000: Continuation and bifurcation software for ordinary differential equations with HOMCONT," Technical Report, Concordia University, 2002.
- ²⁴V. Astakhov and V. Anishchenko, *Nonlinear Dynamics in Circuits*, edited. L. M. Pecora (World Scientific, Singapore, 1995), pp. 55–88.
- ²⁵A. Koseska, E. Volkov, and J. Kurths, *Chaos* **20**, 023132 (2010).
- ²⁶Y. Yamaguchi and H. Shimizu, *Physica D* **11**, 212 (1984).
- ²⁷R. E. Mirollo and S. H. Strogatz, *J. Stat. Phys.* **60**, 245 (1990).
- ²⁸B. Ermentrout, *Physica D* **41**, 219 (1990).
- ²⁹D. V. Ramana Reddy, A. Sen, and G. L. Johnston, *Phys. Rev. Lett.* **80**, 5109 (1998).
- ³⁰D. V. Ramana Reddy, A. Sen, and G. L. Johnston, *Physica D* **129**, 15 (1999).
- ³¹F. M. Atay, *Phys. Rev. Lett.* **91**, 094101 (2003).

- ³²F. M. Atay, *Physica D* **183**, 1 (2003).
- ³³R. Karnatak, R. Ramaswamy, and A. Prasad, *Phys. Rev. E* **76**, 035201(R) (2007).
- ³⁴E. Ullner, A. Zaikin, E. I. Volkov, and J. Garcia-Ojalvo, *Phys. Rev. Lett.* **99**, 148103 (2007).
- ³⁵Y. Zhai, I. Z. Kiss, and J. L. Hudson, *Phys. Rev. E* **69**, 026208 (2004).
- ³⁶R. Herrero, M. Figueras, J. Rius, F. Pi, and G. Orriols, *Phys. Rev. Lett.* **84**, 5312 (2000).
- ³⁷D. V. R. Reddy, A. Sen, and G. L. Johnston, *Phys. Rev. Lett.* **85**, 3381 (2000).